

Homogeneous Regions of Precipitation Trends Across the Amazon River Basin, Determined From the Global Precipitation Climatology Centre - GPCC

David Figueiredo Ferreira Filho (✉ davydferreira@gmail.com)

Federal University of Para

Francisco Carlos Lira Pessoa

Federal University of Para

Article

Keywords: Mann-Kendall, Sen's slope, Precipitation Indices, Amazon River Basin, Precipitation Variations

Posted Date: November 3rd, 2022

DOI: <https://doi.org/10.21203/rs.3.rs-2202483/v1>

License:  This work is licensed under a Creative Commons Attribution 4.0 International License.

[Read Full License](#)

Additional Declarations: No competing interests reported.

HOMOGENEOUS REGIONS OF PRECIPITATION TRENDS ACROSS THE AMAZON RIVER BASIN, DETERMINED FROM THE GLOBAL PRECIPITATION CLIMATOLOGY CENTRE - GPCC

David Figueiredo Ferreira Filho^{1,*}, Francisco Carlos Lira Pessoa²

¹ - Environmental Engineer, Phd in progress in Civil Engineering - PPGEC, Federal University of Pará - UFPA; Campus Belém, Av. Augusto Corrêa, Neighbourhood Guamá s/n, CEP: 66075-110, Belém, State of Pará, Brazil, davydferreira@gmail.com, <https://orcid.org/0000-0002-5890-3515>

² - Sanitary and Environmental Engineer, PhD in Amazon Natural Resources Engineering - PRODERNA, Federal University of Pará - UFPA; Campus Belém, Av. Augusto Corrêa, Neighbourhood Guamá s/n, CEP: 66075-110, Belém, State of Pará, Brazil, fclpessoa@ufpa.br, <https://orcid.org/0000-0002-6496-9043>

*Corresponding author: David Figueiredo Ferreira Filho, davydferreira@gmail.com

1 **Abstract:** Spatiotemporal patterns of precipitation are influenced by complex interactions between
2 climate and land cover changes, such as deforestation, fires and droughts. The Amazon River Basin has
3 local and global impacts in regard to the hydrological cycle; therefore, it is fundamental to understand
4 how precipitation patterns and intensity are changing. The aim of this study was to analyze precipitation
5 trends and form homogeneous regions of precipitation trends in the Amazon River Basin using data from
6 the meteorological satellite Global Precipitation Climatology Centre (GPCC), applying nonparametric
7 methods (Mann-Kendall, Spearman and Sen's slope) and fuzzy C-means to identify specific regions that
8 are undergoing changes in hydrological patterns. The results show changes in the behavior of rainfall over
9 time and in the intensity of the events. The statistics applied to form clusters resulted in 6 well-divided
10 homogeneous groups, each with unique characteristics. Specifically, the central-southern areas of the
11 basin showed negative precipitation trends (-1.17 mm/year) forming a homogeneous region (RH 1), while
12 in the northern region, there was an increasing trend in precipitation (2.73 mm/year). In general, over the
13 37 years studied, the wet areas have tended to become wetter and the dry areas drier. Other homogeneous
14 regions had their own results and unique characteristics, which are in agreement with other studies, such
15 as those in Porto Velho, Rondônia, where this area had a diagonal pattern of precipitation decrease.

16 **Keywords:** Mann-Kendall; Sen's slope; Precipitation Indices; Amazon River Basin; Precipitation
17 Variations.

18

19 1. INTRODUCTION

20 The Amazon River basin, located in South America, contains approximately 60% of the world's
21 tropical forests, according to a study by Arvor et al. (2017), which play a vital role in regulating climate
22 circulation patterns, which in turn contribute to local and global biodiversity and sustain ecosystems
23 (Haghtalab et al. 2020).

24 The current ecosystems have suffered several impacts, especially in the last three decades, due to
25 increased human activities in the region, examples being the development of infrastructure, inadequate
26 extraction of natural resources, advance of deforestation, vegetation suppression, replacement of forests
27 for pastures, expansion of the agricultural sector, among others (Costa and Pires 2010; Davidson et al.
28 2012).

29 Impacts such as these alter land use patterns causing pressures on soils and riverbeds,
30 consequently the climate and the hydrological water cycle (Longobardi et al. 2016). In addition, they
31 affect land surface characteristics such as reflectance index and roughness (Albedo), which directly alter
32 surface energy and water flows (Haghtalab et al. 2020).

33 Actions such as reductions in surface roughness due to the extraction of vegetation cover
34 unbalance the regional hydroclimate, causing thermal changes. In contrast, the preservation of forests
35 helps maintain the climate and soil in the region (Walker et al 2009; Khanna et al 2017).

36 Although much debated, the effects of vegetation cover removal on climate circulation patterns
37 are also affected by climatic phenomena such as the El Niño-Southern Oscillation (ENOS) and the Pacific
38 Decadal Oscillation (PDO), as discussed by Marengo and Espinoza 2016.

39 ENOS events have been recurrent in recent years, aggravating droughts and intensifying floods
40 (Laurance et al. 2002). Thus, one of the influences that precipitation has suffered in recent years may be
41 related to changes in sea surface temperatures, the occurrence of ENOS events, atmospheric circulation
42 phenomena such as SACZ and ITCZ, and the removal of vegetation cover (Marengo and Espinoza 2016;
43 Khanna et al. 2017).

44 In this way, quantifying changes in the variability of precipitation in the Amazon River basin
45 region becomes essential to analyse the effects produced by such anomalies, since precipitation is non-
46 uniform and if studied at smaller scales, the influence of other factors can be perceived, resulting in
47 greater spatial and temporal variability (Laurance et al. 2002; Funatsu et al 2012).

48 In 2004, Marengo (2004) published a scientific study about precipitation trends in the Brazilian
49 Amazon, using meteorological stations. According to the research data, there was a strong negative trend
50 in precipitation, based on the historical series from 1929 to 1998. However, Satyamurty et al. (2010),
51 using multidecadal station datasets, found only weak rainfall trends, a fact that further makes studies of
52 trends in the region an important factor in understanding rainfall behaviour.

53 As science advances, studies in the region have also advanced. Debortoli et al. (2015) detected
54 more negative than positive rainfall trends in deforested regions in Amazonia during the transition months
55 between the wettest and wettest seasons. According to the study, the relationship between deforestation
56 and rainfall resulted in a reduction of approximately 88% in the rainfall records of the pluviographs.
57 However, Almeida et al. (2017) found no trends between the period 1973 to 2013 for the same area, with
58 the same data source. However, it is known that in the Amazon region, the recorded data often present
59 measurement problems, failures in their records and/or absences, a fact that some studies have addressed
60 the use of meteorological satellite data.

61 According to Paca et al. (2020), the increased use of remote sensing products and global
62 precipitation datasets are suitable for hydrological studies, especially in remote, unmeasured and data-
63 deficient areas. For this reason, Salviano et al. (2016) used monthly precipitation data from the Climatic
64 Research Unit (CRU), and analysed the trends in Brazil, and found some changes in rainfall behaviour.

65 Silva et al. (2018) also used reanalysis data. For the present study, the data used were from the
66 Tropical Precipitation Measurement Mission (TRMM), from 1998 to 2015. According to the authors'
67 results, 92.3% of the Brazilian Amazon had no rainfall trends during the historical series, while 4.2% had
68 significant negative trends ($p \leq 0.05$) and 3.5% had positive trends.

69 Thus, the objective of this study was to analyze rainfall trends for the Amazon River Basin,
70 using the non-parametric methods of Mann-Kendal, Spearman and Sen's Slope, with the aim of

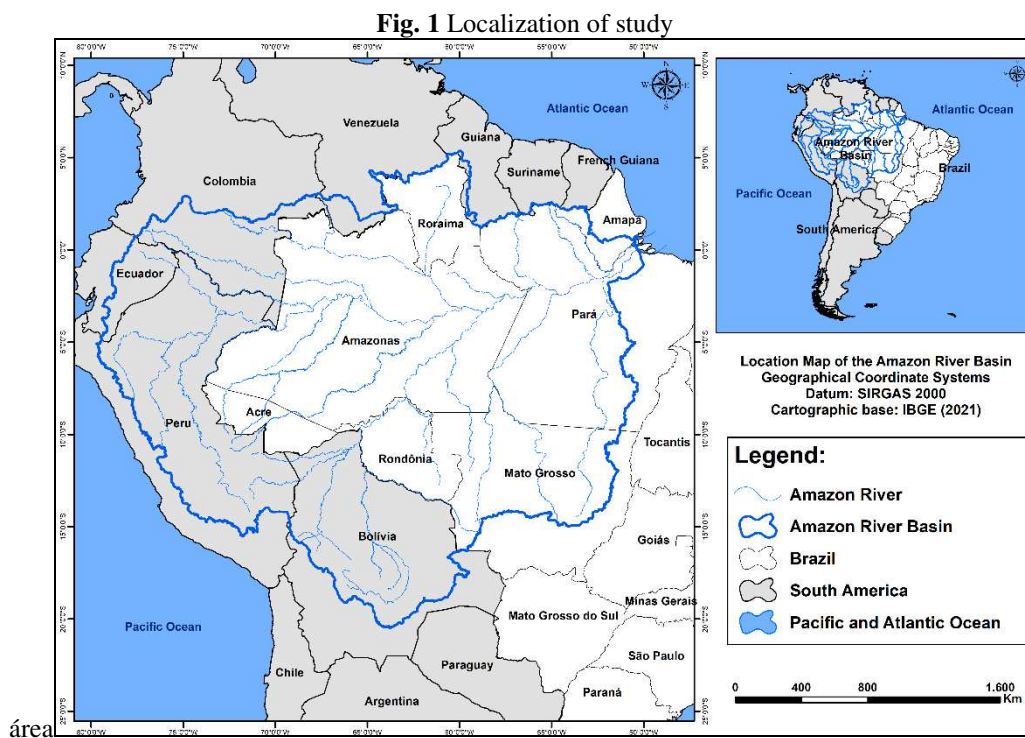
71 identifying and forming homogeneous groups of rainfall trends, through the Fuzzy C-Means technique,
72 using meteorological satellite data provided by the Global Precipitation Climatology Centre (GPCC), for
73 the period 1982 to 2021, with a focus on identifying specific regions that are undergoing changes in
74 hydrological patterns and that can serve as potential aids in studies about the knowledge of the area and
75 its impacts on the regional hydrological cycle.

76 2. MATERIALS AND METHODS

77 2.1. Area of study

78 The present study was developed for the Amazon River Basin (HBRA), in South America (Fig.
79 1), which has a territorial extension of approximately 7,050,000 km². The HBRA is composed of 7
80 Brazilian Federative Units, namely: Acre, Amazonas, Rondônia, Roraima, Amapá, Pará and Mato
81 Grosso, and part in other South American countries, such as Bolivia, Peru, Ecuador, Colombia,
82 Venezuela, Republic of Guyana, Suriname and French Guiana.

83



84

área

85

Source: Authors

86 The Amazon Basin is considered the most productive basin in South America, with the Amazon
87 River as its main river, contributing approximately 15% of the average global runoff, and having two
88 large tributaries, the Negro and Solimões Rivers (Campos 2004; Silva 2013). Characteristic with high
89 rainfall volumes, it has a high correlation with ENOS events (Filizola 1999; Marengo et al 2011).

90 Tomassela et al. (2013), highlight that the eastern portion of the BiH is influenced by the
91 Intertropical Convergence Zone (ITCZ) and the western portion by the South Atlantic Convergence Zone
92 (SACZ), being characterized by an equatorial type climate, with intense precipitation throughout the year
93 and an average temperature between 24°C and 36°C.

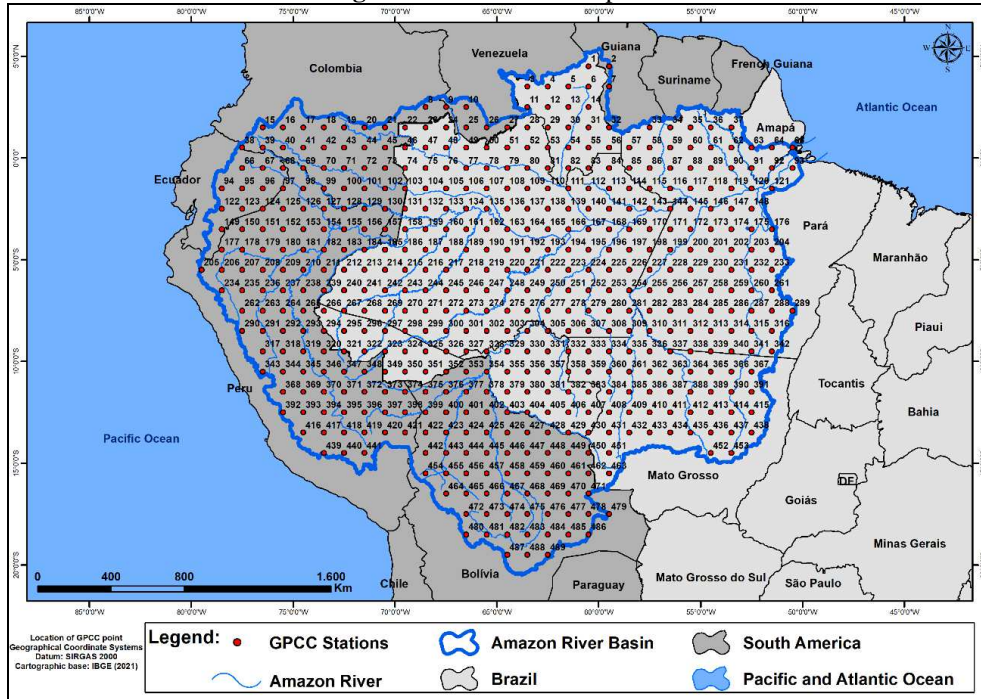
94 2.2. Data selection - Global Precipitation Climatology Centre (GPCC)

95 In this manuscript the GPCC satellite dataset was used. It is one of the most recent and accurate
96 in precipitation estimation and production (Rustemeier et al. 2019).

97 Its data have been frequented in studies of global and regional climatology, and offers itself as an
98 alternative of precipitation measurements, given that, especially in the Amazon, most stations are along
99 the rivers, have faulty observations, some incorrect data, and unevenly distributed, do not obey some
100 criteria established by the World Meteorological Organization (WMO 2008).

101 In this work, we used a grid of 0.5° x 0.5° latitude by longitude (Fig. 2), for a historical series of
102 39 years of precipitation data (1982 - 2021).

Fig. 2 Location of GPCC points



104

105

Source: Authors

106

Thus, it can be observed that there are 486 points in the study area. Where from them will begin the methodological procedures addressed here. Furthermore, satellite precipitation products have the advantages of (1) being uniform and continuous in space and time, (2) reporting values consistently, and (3) covering large areas at global or continental scale (Paca et al. 2020).

107

108

As addressed, the poor coverage within the study region (Delahaye; Kirstetter; Dubreuil 2015) and a new approach with a distinct data source from other studies, led to the use of this meteorological satellite in this study.

109

110 **2.3. Nonparametric Methods**

111

Nonparametric tests are so called because they are distribution-free statistics, not constrained by assumptions about population distribution; consequently, they can easily accommodate data that have a wide range of variation. Unlike parametric statistics, these distribution-free tests can be used with both quantitative and qualitative data (Scheff 2016).

112

113

In this sense, the nonparametric methods used in this work attempted to verify the occurrence of precipitation trends in the study area using the nonparametric tests of Mann-Kendall, Spearman and Sen's slope estimators.

114

115

Thus, tests such as Mann-Kendall, Spearman and Sen's slope are used to analyze the trends of various climatological variables to collaborate with the planning of water resources, as in a study conducted by Ishihara et al. (2014), Loureiro et al. (2015), Menezes and Fernandes (2016) and Asfaw et al. (2018).

116

117

These methods start from the principle of elaborating a hypothesis based on the probabilistic behavior of a series of one or more variables, defining a null hypothesis (H0) and another alternative hypothesis (Ha), such that the rejection of the null hypothesis depends on the type of test applied and the significance level (α) adopted (Loureiro et al. 2015).

118

119

Then, because they are two-tailed tests, to reject the null hypothesis (H0) and accept the alternative hypothesis (Ha), it is necessary that the absolute values of the methods are higher or lower than $Z_{\alpha/2}$. Thus, this paper adopted a 95% confidence level and 5% significance level, i.e., $\alpha = 5\%$, $Z = \pm 1.96$ (Salviano et al. 2016).

120

121

For Pandey and Khare (2018), these methods did not require a normal distribution of data; with this, they become suitable for temporal trend analysis in climate and hydrological data series.

122

123

124

135 Therefore, the Mann-Kendall nonparametric test is a test used to identify changes in climate in
 136 time series studies, where the values must be independent and the probability distribution must always
 137 remain the same (Ely and Dubreuil 2017). Mann (1945) and Kendall (1975) defined the statistic of the
 138 method as the statistical variable S for a series of data (n) calculated from the sum of signs (sgn) of the
 139 difference, pairwise, of all values of the series (xi) in relation to the values that are forthcoming to them
 140 (xj), expressed in Equations 1 and 2:

$$S = \sum_{i=1}^{n-1} \sum_{j=i+1}^n \text{sgn}(x_j - x_i) \quad \text{Equation (1)}$$

$$\text{sgn}(x_j - x_i) = \begin{cases} +1; & \text{se } x_j > x_i \\ 0; & \text{se } x_j = x_i \\ -1; & \text{se } x_j < x_i \end{cases} \quad \text{Equation (2)}$$

141 When n is greater than or equal to 10, the variable S can be compared with a normal distribution,
 142 in which its variance, Var (S), can be obtained from Equation 3, where ti represents the number of
 143 repetitions of an extension i.

$$\text{Var}(S) = \frac{n(n-1)(2n+5) - \sum_{i=1}^p t_j(i)(i-1)(2i+5)}{18} \quad \text{Equation (3)}$$

144 P is the number of linked groups and tj is the number of data values in the group; thus, the values
 145 of Var (S) and S are used to calculate the ZMK, obtaining positive, negative or null trend parameters as a
 146 result.

$$\text{ZMK} = \begin{cases} \frac{S-1}{\sqrt{\text{VAR}(S)}} & \text{se } S > 0 \\ 0 & \text{se } S = 0 \\ \frac{S+1}{\sqrt{\text{VAR}(S)}} & \text{se } S < 0 \end{cases} \quad \text{Equation (4)}$$

147 Thus, similar to the Mann-Kendall test, Spearman's nonparametric test is usually used to verify
 148 trends in temporal series (Abdul and Burn 2006; Partal and Kahya 2006).

149 This method is based on the calculation of the correlation coefficient in order (ranks) of x and y,
 150 related pair by pair. Thus, according to Equation 5, the Spearman coefficient is calculated as follows:

$$P_s = 1 - \frac{6}{n^3 - n} \sum_{i=1}^n (R_{xi} - R_{yi})^2 \quad \text{Equation (5)}$$

151 Where Rxi is the order of element Xi in the series in natural order; Ryi is the order of element Yi
 152 in the series in increasing form; and n is the number of elements of the sample. With this, the coefficient
 153 is a random variable with a symmetrical distribution, with the mean and variance shown in Equation 6:

$$E(ps) = 0 \text{ e } \text{Var}(ps) = \frac{1}{n-1} \quad \text{Equation (6)}$$

154 Thus, statistically, the test is given by Equation 7 below:

$$T_{n-2} = \sqrt{\frac{(n-2)(ps^2)}{(1-ps^2)}} \quad \text{Equation (7)}$$

155 Finally, Sen's slope test, which was proposed by Sen (1968) and was improved by Hirsch et al.
 156 (1984) and according to the authors Portela et al. (2011) and Tao et al. (2014), is estimated by means of
 157 the Q statistic, according to Equation 8:

$$Q_{ij} = \frac{X_j - X_i}{j - i} \quad \text{Equation (8)}$$

158 Where Xi and Xj are values of the variable under study in years i and j, respectively. Thus,
 159 positive or negative results for Q indicate increasing or decreasing trends, respectively. If there are n
 160 values in the series analyzed, then the number of estimated pairs of Q is given by the equation below:

$$N = \frac{n * (n - 1)}{2} \quad \text{Equation (9)}$$

161 Therefore, Sen's slope estimator is the median of the N values of Qij, being insensitive to outliers
 162 and nonexistent data, demonstrating a simulated measure of the trends that may come to exist in a
 163 historical data series (FERRARI, 2012).

164 2.4. Fuzzy C-Means

165 To identify the homogeneous regions of precipitation trends, the non-hierarchical Fuzzy C-
 166 Means method proposed by Dunn (1973), then improved by Bezdek (1981) and introduced into science
 167 by Zadeh (1965) was applied. The method is also recognised as Fuzzy (Aguado and Catanhede 2010).

168 The variables selected to introduce in the method were Geographic Coordinates (Latitude and
 169 Longitude), Mean Annual Precipitation, the results of Sen's Slope method, Euclidean Distance, and fuzzy
 170 parameters.

171 The fuzzy is known as fuzzy clustering, in other words, is characterized by the basic idea that in
 172 a data set $X = \{x_1, x_2, \dots, x_n\}$ is divided into groups p, and the results of clustering are expressed by the
 173 degrees of pertinence, so that, each element can belong to a single group or more.

174 In this way, an element belongs or not to a given set, where a universe U and a particular element
 175 x belong to U and the degree of belongingness $\mu_A(x)$ with respect to a set A belongs to U, such that the
 176 function $\mu_A(x) = U = \{0,1\}$ is called the characteristic function.

177 To generate the partition of clusters, it is necessary to minimise an equation function through an
 178 iterative algorithm, which indicates the degree of pertinence of an element belonging to a particular
 179 cluster (Xu and Wunsch 2005). Through an assumption, the algorithm is formed, so that a database $X =$
 180 $\{x_1, x_2, x_3, \dots, x_n\}$, where each point $x_k, k=(1,2,3, \dots, n)$ is a vector \mathbb{R}^p , n is the total data of the database X
 181 and \mathbb{R}^p represents a p-dimensional space of the real numbers, which can be one-dimensional, two-
 182 dimensional and/or three-dimensional (Bloch 2005). Thus, the partition matrix for the domain X is
 183 arranged through Equation 10:

$$Mfnc = \left\{ U \in Ucn : U_{ik} \in [0,1], \sum_{i=1}^c U_{ik} = 1, 0 < \sum_{k=1}^n U_{ik} < n \right\} \quad \text{Equation (10)}$$

184 Where Ucn is the group of real matrices $c \times n$; c is the number of clusters that will be found,
 185 arranged $2 \leq c \leq n$; U is the fuzzy partition matrix for the domain X; and U_{ik} is the degree of pertinence of
 186 x_k in Cluster i. In this way, if you sum all the pertinence degrees U_{ik} for a given data, their sum should
 187 always be equal to 1, and the sum of all the pertinence degrees should be in the range between 0 and n.

188 As the fuzzy is fuzzy, at each new iteration new centroids are produced, in this way, the task of
 189 generating an indicator that helps to check the convergence between the data is assigned to the objective
 190 function (J), defined by means of Equation 11 below:

$$J = \sum_{i=1}^n \sum_{j=1}^p (U_{ik})^m * d(X_k, C_j)^2 \quad \text{Equation (11)}$$

191 Where n is the number of data points; p is the number of clusters; U_{ik} is the degree of pertinence
 192 of sample X_k to j=th cluster; m is the fuzzy parameter; d is the Euclidean distance between X_k and C_j ; X_k
 193 is the data vector, where $i=1, 2, \dots, n$ represents a data attribute; and C_j is the center of a fuzzy cluster.

194 Then, the objective function J is minimized, and the pertinence degrees U_{ik} are generated
 195 according to Equation 12:

$$U_{ik} = \left[\sum_{k=1}^c \left(\frac{d(X_k, C_j)}{d(X_k, C_j)} \right)^{2/(m-1)} \right] \quad \text{Equation (12)}$$

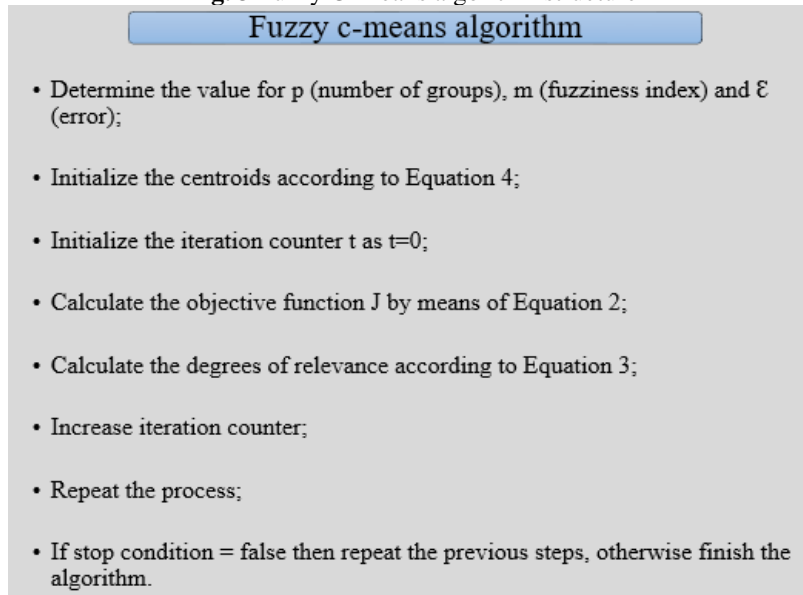
196 C_j is a vector called a centroid (Pedrycz and Vukovich 2004), which can be obtained through
 197 Equation 13:

$$C_j = \frac{\sum (U_{ik})^m X_k}{\sum (U_{ik})^m} \quad \text{Equation (13)}$$

198 As the degrees of pertinence are defined by the highest degree of correlation, the algorithm needs
 199 some execution steps (Fig. 3) (Nascimento et al 2000). It is necessary to establish some rules, according
 200 to Bezdek (1992), and in this manuscript, it was adopted some following those applied by Gomes, Blanco
 201 and Pessoa (2018).

202

Fig. 3 Fuzzy C-Means algorithm structure



203

204

Source: Bezdek (1992)

205

2.5. Validation Indices

206

All grouping processes produce a solution even when the original data do not have any substructures (Tan; Steinbach; Kumar 2005).

208

The C-means method, because it is a free choice method of group formation, can generate several solutions, which are reapplied several times to avoid local minima of the objective functions, and to minimize these questions, validation indices are used to evaluate the results generated by clustering algorithms (Halkidi; Batistakis; Vazirgiannis 2002).

212

Therefore, in this work, validations were performed through the Pakhira-Bandyopadhyay-Maulik (PBM), silhouette (SIL), Dunn (D), Davies Bouldin (DB) and Xie Beni (XB) indices. Table 1 shows the indices and their equations.

213

214

Table 1 Validation rates and their equations

Index	Source	Equation
Davies Bouldin (DB)	PAKHIRA et al. (2004).	$DB = \frac{1}{K} * \sum_{i=1}^K Ri, qt$
Silhouette (SIL)	ROUSSEAW (1987)	$s(i) = \frac{bi - wi}{\max (bi, wi)}$
PBM	PAKHIRA et al. (2004).	$PBM = (\frac{1}{k} * \frac{E1}{Ek} 8 * Dk)^2$
Dunn (D)	PAKHIRA et al. (2004).	

$$Vd = \min_{1 \leq s \leq K} \left\{ \min_{1 \leq t \leq K, t \neq s} \left\{ \frac{\partial i(Gs, Ct)}{\max_{1 \leq k \leq K} \Delta j(Gk)} \right\} \right\}$$

Xie Beni (XB)

PAKHIRA et al. (2004).

$$S = \frac{Jm}{n * (dmin)^2}$$

215 The use of these indexes is necessary because, according to Tan, Steinbach and Kumar (2005),
 216 all clustering processes produce a solution, even when the raw and original data do not have any
 217 substructures. The C-Means method is a free choice method of group formation, and to avoid erroneous
 218 decisions, the applicability of validation indexes become of great value to enrich the results generated by
 219 the clustering algorithms (Halkidi; Batistakis; Vazirgiannis 2002).

220 There are two strands as to the applicability of the indices, some minimize their coefficient to
 221 obtain the best result, such as Davies Bouldin and Xie Beni, and others maximize, such as Dunn, Silhouett
 222 and PBM.

223 The PBM index has as main objective to maximize the index to obtain the optimal number of
 224 cluster, in other words, the maximum value is selected for the best partition (Pakhira et al. 2004). As for
 225 the Silhouett method (Rousseeuw 1987), the width of the silhouette evaluates the quality of the clustering,
 226 considering both compactness among data (distance between data points within the same group) and
 227 separation (distance between data points in two neighbouring groups).

228 Dunn's method (D) (Dunn 1974) is defined as S and T, two non-empty subsets in the RN. The
 229 Davies Bouldin (DB) index (Davies and Bouldin 1979) is a function of the ratio of the sum of the
 230 dispersion within the cluster and the separation between clusters. The dispersion in the i-th cluster is
 231 calculated according to its equations. In turn, the Xie Beni (XB) index (Xie and Beni 1991) is considered
 232 a fuzzy clustering index, from which its generalised version is obtained through its equation.

233 3. RESULTS AND DISCUSSION

234 3.1. Spatial Analysis and Precipitation Trends

235 This study is based on several international articles that addressed topics on hydrology,
 236 climatology and meteorology, and which adopted data measured by meteorological satellites as a data
 237 source.

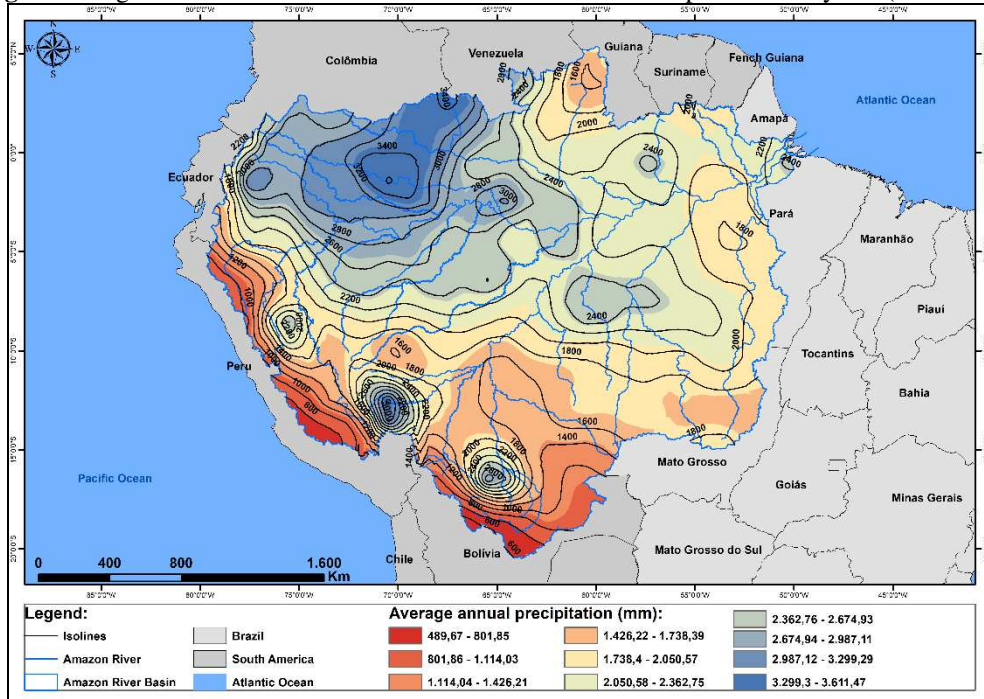
238 In recent years, satellites have improved, becoming the primary choices for some studies, such as
 239 those by Getirana et al. (2011) and Limberger and Silva (2018), the latter being from the GPCC that is the
 240 most suitable for analyzing precipitation in the Amazon.

241 In a recent study developed by Haghtalab et al. (2020), the GPCC, together with the CHIRPS
 242 satellite, are the ones that best estimate satellite precipitation data for Amazonia, which was confirmed in
 243 a study by Funk et al. (2015).

244 As an example of its expansion and improvement, in the work developed by Schneider et al.
 245 (2014), the GPCC had a database with 67,200 monitoring stations, and in work developed by Rustemeier
 246 et al. (2019), it already had a base with more than 75,000 stations, confirming its improvement in recent
 247 years. Fig. 4 shows the results obtained in the spatialization of mean annual precipitation in the Amazon
 248 River Basin for a period of 39 years (1982–2021).

249

Fig. 4 Average annual rainfall over the Amazon River basin for a period of 39 years (1982-2021)



250

251

Source: Authors

252

The highest precipitation regime was found in the northwestern part of the study area, in Colombia and in part of Amazonas State in Brazil, ranging from 2,000 mm to rates above 3,500 mm.

254

The lowest precipitation records were distributed along the Andes Mountains, in Ecuador and Peru, in the subbasin of the Solimões River, and in Bolivia in the subbasin of the Madeira River. These results are similar to those in the studies by Villar et al. (2009), Arvor et al. (2017) and Paca et al. (2020).

257

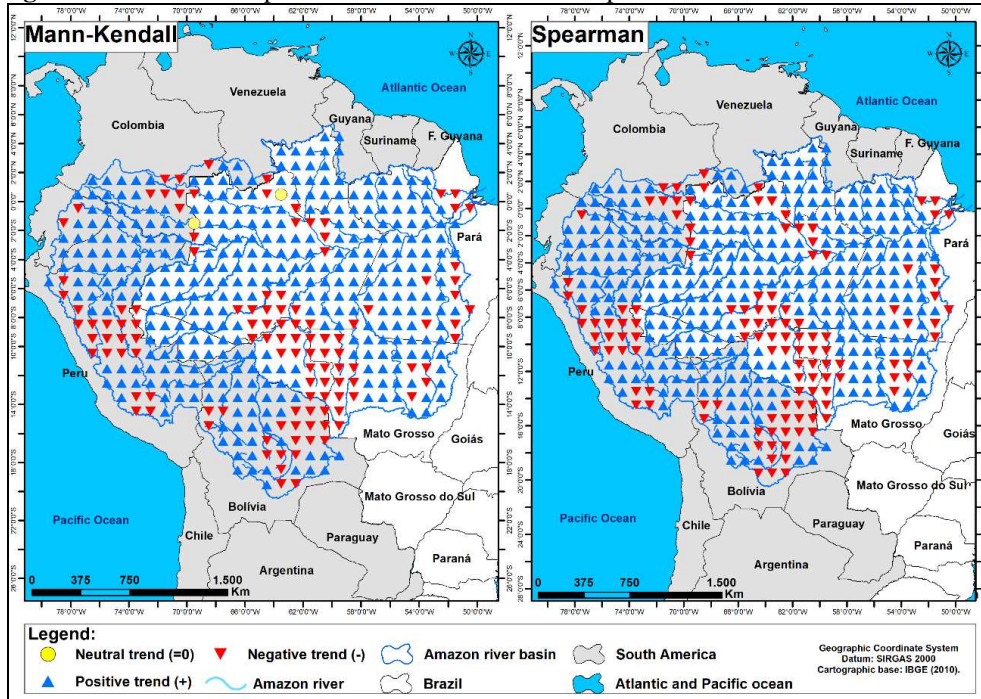
As the main objective of this study was to analyze the precipitation trends in the basin for each point of the GPCP grid, the 3 tests proposed in this study were applied. Thus, a total of 1464 tests were performed, where the objective was to analyze the precipitation trend in the study area.

260

Therefore, the Mann-Kendall and Spearman tests were spatialized (Fig. 5) for the best visualization of the behavior of trends in the study region.

261

Fig. 5 Results of the nonparametric Mann-Kendall and Spearman tests for each GPCC station



263

264

Source: Authors

265

266

267

268

Of the 488 stations, the Mann-Kendall test showed 368 stations with positive rainfall trends and 2 stations with neutral trends. equal to 0 (zero) and 118 with negative trends. In the Spearman test, 365 stations showed positive trends and 123 showed negative trends, and there were no null records in this test.

269

270

271

Therefore, analyzing the results presented in Figure 5, a negative trend was noted in the central portion of the study area; more specifically in the arc of deforestation of the Brazilian Legal Amazon, similar to the results in the study by Lira (2019).

272

273

274

275

276

277

278

These negative trends may have been associated with the removal of native vegetation cover, a fact that is a determinant of precipitation. According to a study by Haghtalab et al. (2020), these areas had annual decreases 30% more frequently than the rest of the time series, and this detection of change points had abrupt reductions in daily precipitation in these regions after 1998, 1995, and 1992, which were all ENOS years, which, combined with anomalous warming in the Atlantic Ocean, may have caused less precipitation across the basin.

279

280

281

Nevertheless, in this central portion near Porto Velho, there was a significant increase in extreme drought events in 1989, with the detection of significant change points in 1997, which was a year of extreme drought.

282

283

284

285

286

287

Another important result to be highlighted is related to the mouth of the Amazon River, where both tests showed negative trend results, which could have changed the entire local climatology, causing responses in changes in the hydrological cycle and climate change, generating a decrease in runoff, and changing the total precipitation and quantities and temporal distribution of runoff, as well as the amount of water, changes in the quotas of the river, hydrodynamics and the entire trophic structure of biological communities (Tejadas et al. 2016).

288

289

290

291

In tropical rivers, ecological and climatic patterns regulate habitat preference, resource availability, and ecological structure (Braga et al. 2012; Correa and Winemiller 2014; Mortillaro et al. 2015; Prudente et al. 2016); for this reason, investigations regarding climate change are necessary in several studies.

292

293

294

295

Another example related to climate influence is fish reproduction, which has been highlighted in the Amazon region, where the onset of rainfall has been related to the formation of dry or floodable areas, resulting in an increase or reduction in food availability, similar to studies by Sánchez-Botero and Araújo-Lima (2001) and Leite et al. (2006).

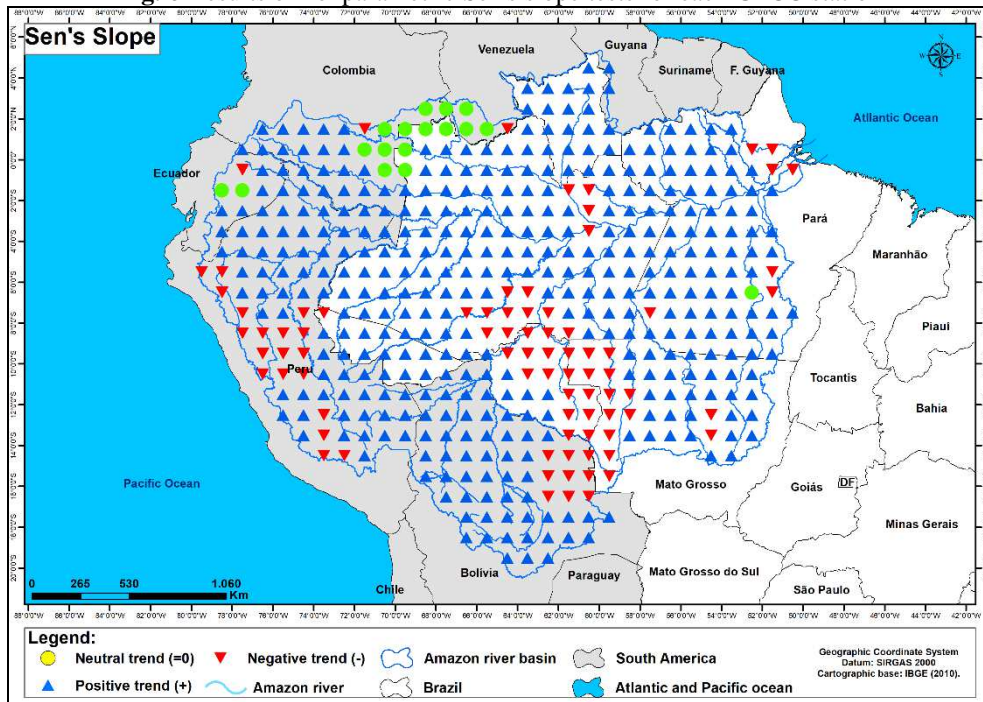
296 In the Andean portion, the study by Haghtalab et al. (2020) showed that for 2001, only one site
297 had a significant increasing/drying trend (region G in their study and a region with a negative trend in this
298 study), and the general trend of increase was clearly recognizable. In this study, the results were different,
299 showing that there was a decrease presented by the two tests applied, which indicates that there is an
300 inconsistency in the data.

301 In the northernmost Andean portion, the results presented by the 2 tests showed trends of
302 increasing precipitation; according to Haghtalab et al. (2020), this region showed that precipitation during
303 the dry season doubled after 2012 compared with the previous average of 11 extreme events.

304 Thus, Sen's slope was applied, which is a nonparametric method that has been used to quantify
305 the magnitude of the precipitation slope (changes per unit time) as opposed to the step count of MK's tau
306 and Spearman's rho statistics. Therefore, Fig. 6 illustrates the results of the statistics applied by Sen's
307 method.

308

Fig. 6 Results of nonparametric Sen's slope tests for each GPCP station



309

310

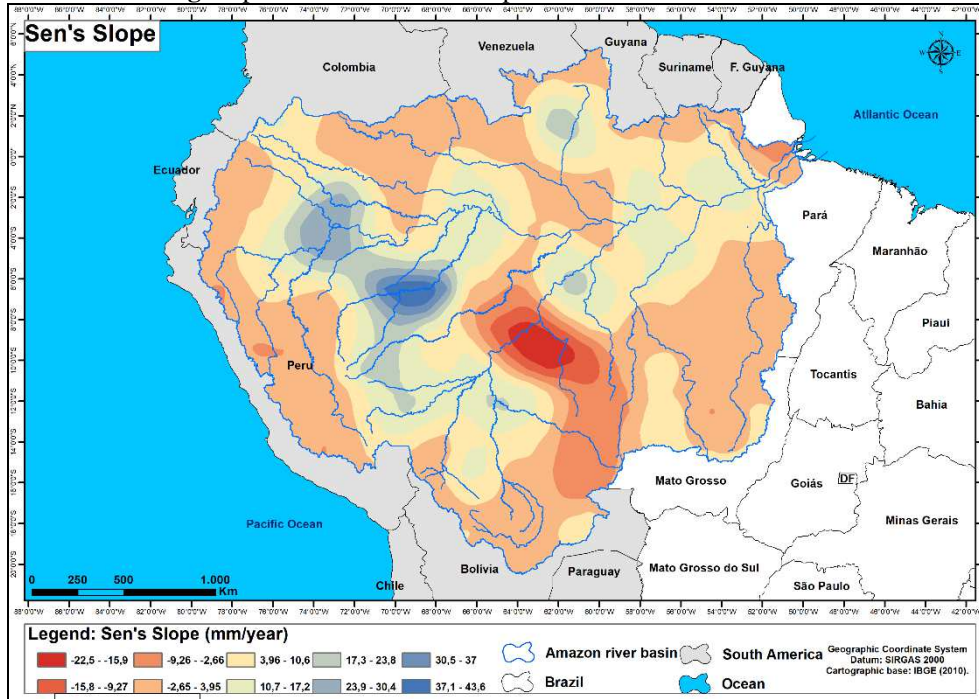
Source: Authors

311 It can be noted that the three tests applied in this study showed similar results; however, stations farther
312 north of the study area based on the Mann-Kendall and Spearman methods showed trends in rainfall, but
313 Sen's estimator showed null trends, demonstrating that there was no increase or decrease in rainfall
314 volumes in recent years.

315 Another important fact is that the central portion of the hydrographic basin showed a negative
316 trend in the three methods, and as mentioned previously, this fact was related to deforestation in this area,
317 which accelerated significantly during the 1990s and early 2000s in the Brazilian Amazon, reaching an
318 annual rate of 27,423 km² in 2004 (INPE 2004).

319 Furthermore, major changes in the regional use and occupation context have been strongly
320 associated with deforestation and forest degradation in the region (Monte-Mor 2013), thus affecting the
321 local climate system (Song et al. 2015). Thus, as the objective of Sen's method is to quantify the trends
322 throughout the year, the spatialization of the values obtained from the stations was made (Fig. 7).

Fig.7 Spatialization of Sen's slope for the Amazon River Basin



324

325

Source: Authors

326

327

328

329

Most of them show statistically significant increasing trends, with the exception of the central part of the basin, whose negative trend was very strong (between -22.5 and -2.66 mm/year), which could indicate a water crisis in this location, which, according to Haghtalab et al. (2020), suffered from a drought in 2015, unlike in 1993 when the region had high humidity.

330

331

332

333

334

335

Other data presented are in the area of Santa Cruz de La Sierra, Bolivia, indicating strong results of negative precipitation trends, ranging from -9.26 mm/year to -2.66 mm/year, demonstrating a considerable decline in precipitation throughout the year, where Haghtalab et al. (2020) stated that there was a sharp decline to 2.2 mm/day after 2016, increasing the number of dry days during the dry season by 0.3 days/year, or 11 days in total during the 37 years analyzed, with extreme rates for these years and for 1984, 1988 and 2011.

336

337

338

339

The mouth of the Amazon River presented a negative trend, and by means of Sen's slope test, it was verified that it presented a marked negative trend, between -15.9 mm/year and -22.5 mm/year. Considering a 10-year estimate, precipitation values for this region can change considerably, decreasing by more than 150 mm.

340

341

342

Aceituno (1988), Marengo and Hastenrath (1993), CPTEC (1998) and Marengo et al. (2000) showed a tendency of decreasing precipitation in the entire northern Amazonian area, especially during very intense El Niño years, such as 1982–83 and 1997–9, which was evidenced in this research.

343

344

345

346

According to Nogueira (2008), the negative anomalies of precipitation that occurred in 1982–83 indicate that anomalous warming in the equatorial East Pacific reduced rainfall at the mouth of the Amazon River, and this warming reached up to 5 °C during the evolution of the El Niño of 1982–83 and the El Niño of 1997–1998. In addition to this event, there may have been other influences not studied.

347

348

349

In the border areas between Peru and Colombia, the results of the test showed an increase in local precipitation, in which these regions had large occurrences of extreme rainfall events, when in 2012, there were 29 events, and from this year, their occurrence was well above normal.

350

351

352

353

The bluer bands in the results are located mainly in the state of Amazonas, Brazil. This fact is due to the great conservation of the Amazon biome with areas of difficult access; dense forests, streams, creeks and rivers preserved; low population density; and use and occupation of native soil, thus maintaining high rates of humidity and precipitation over the years.

354

355

One should also highlight the northern portion of the watershed, where there is a greater amount of rainfall per year, whose trend is to continue raining more, which can further change the climatological

normals of the regions formed there, as in studies by Davidson et al. (2012), Lira (2019), and Haghtalab et al. (2020).

3.2. Homogeneous Regions of Precipitation Trends

To form homogeneous regions of precipitation trends, the variables listed in Section 2.4 were introduced in the fuzzy C-means model.

After applying the FCM, the degrees of pertinence of each variable, the number of iterations and the value of the objective function for the different analyses were obtained; thus, to define which is the best grouping, validation indices were again applied to avoid incorrect analyses (Tan; Steinbach; Kumar 2005), generating their respective results for each grouping. The table 2 shows the results of the indices.

Table 2 Best grouping according to the validation indices

Grupo	Indice				
	Davies–Bouldin	Dunn	Silhouette	PBM	Xie-Beni
2	0,1318	0,0569	0,2701	0,6727	0,5882
3	0,1136	0,051	0,3146	0,8425	0,4119
4	0,106	0,051	0,3079	0,8339	0,3524
5	0,1067	0,051	0,2986	0,8312	0,2999
6	0,1173	0,0485	0,3157	0,9084	0,2575
7	0,1283	0,0569	0,2601	0,5416	0,238
8	0,13	0,0569	0,2552	0,4516	0,2222
9	0,1182	0,0569	0,273	0,408	0,1946
10	0,1195	0,061	0,2703	0,3714	0,1712

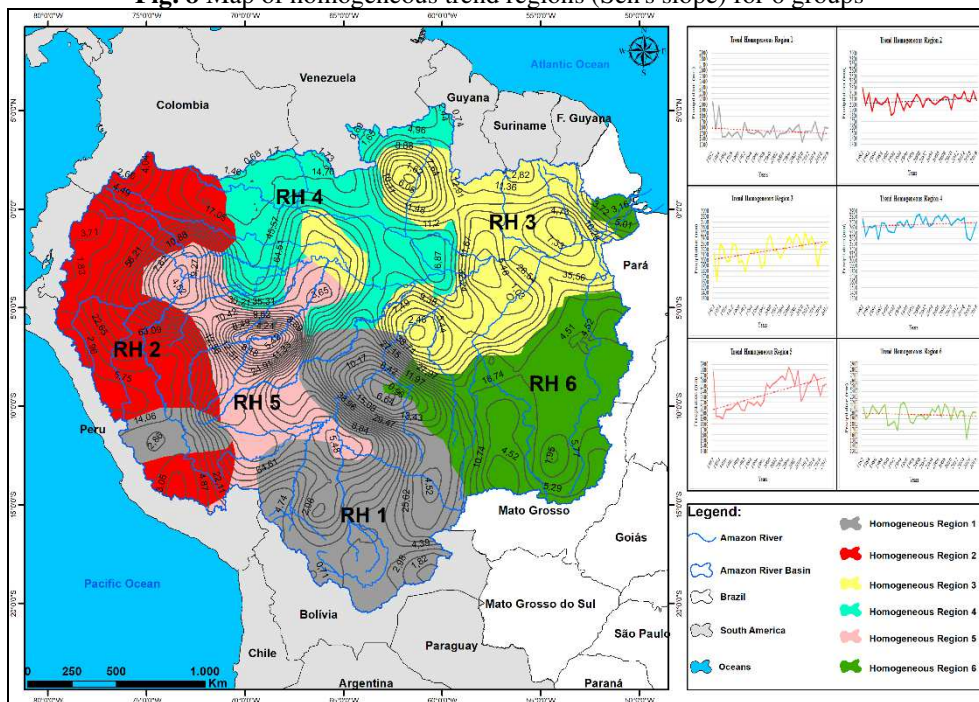
366

The index results demonstrate that variable behaviors are best demonstrated in 6 groupings. These groups formed and validated through these indices represent the homogeneous trend regions (Sen's slope).

Each station had a degree of relevance to a particular group and was spatialized to form homogeneous regions of precipitation trends (Fig. 8).

372

Fig. 8 Map of homogeneous trend regions (Sen's slope) for 6 groups



373

374

Source: Authors

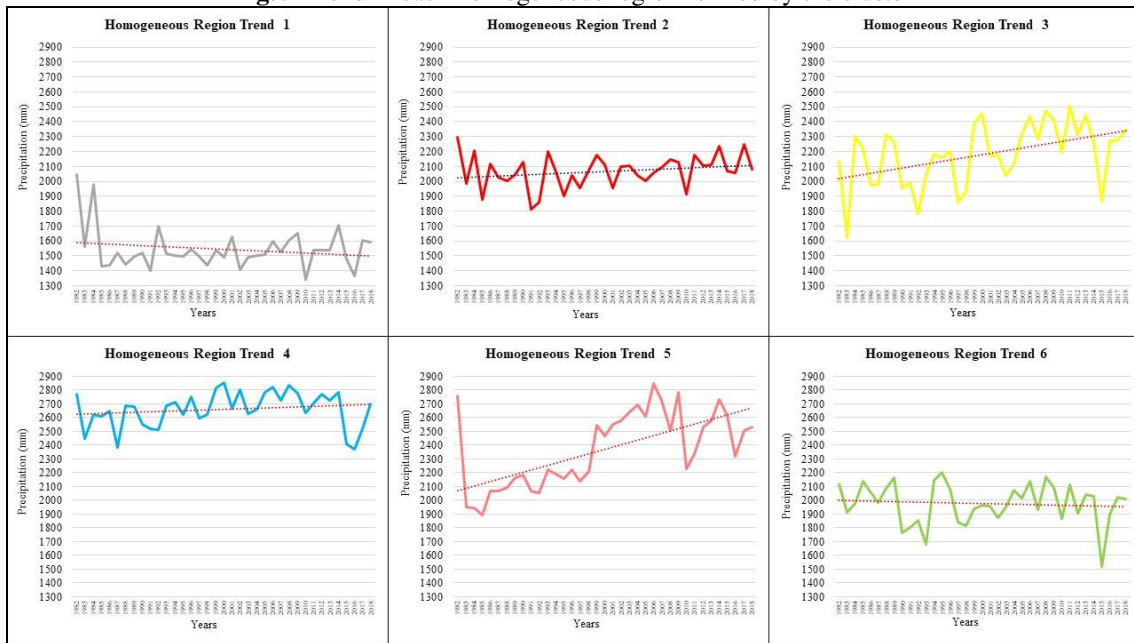
For the groupings, Region 1 presented 83 stations with 17.01%, Region 2 with 81 stations representing 17.60%, Region 3 with 83 stations and 17.01%, Region 4 grouped 80 stations with 16.39%,

376

377 Region 5 with 72 stations and 14.75%, which was the smallest region, and Region 6 with 89 stations and
378 18.24%, which was the largest region.

379 Thus, Fig. 9 represents the behavior of all trends in each region formed.

380 **Fig. 9** Trend in each homogeneous region formed by the cluster



381

382

Source: Authos

383 In homogeneous Region 1, more to the south of the study area, mostly present in the subbasins of the
384 Madeira and Solimões Rivers, presented results of Sen's slope ranging from -15.79 mm/year to 12.82
385 mm/year, with an average annual precipitation of 1545.95 mm and an average elevation of 649 meters,
386 being the last in average precipitation values and the second in terms of elevation, respectively, it is also
387 characterized by a long dry season (Davidson et al. 2012).

388 This presented an average trend with a negative value of -1.17 mm/year, thus the largest with a
389 negative trend, located in the arc of deforestation of the Amazon, and as discussed, the removal of
390 vegetation cover directly impacts rainfall indices, which in turn alters the local climatology.

391 In 1991, 1992, 2002, 2010 and 2016, the lowest average annual precipitation rates were
392 recorded, and in 1992, an ENOS event occurred, with severe drought in this region. By analyzing the time
393 series, one can see the decreasing slope of precipitation, when in 1982, average precipitation rates near
394 1600 mm were recorded. Currently, the trends indicate rates near 1500 mm, whose values may be lower
395 with the occurrence of extreme drought events.

396 These results are consistent with previous studies that identified similar spatial anomalies, such
397 as those in Ronchail et al. (2002), Santos et al. (2015) and Silva et al. (2018).

398 In the case of RH 2, located in the subbasin of the Solimões River, a variation in Sen's slope
399 between -3.19 mm/year and 13.43 mm/year was observed, with an average annual precipitation of
400 2068.47 mm and an average elevation of 1138.89, which was the highest of all regions. Despite being at
401 high elevations, RH 2 did not present low average annual rainfall rates, which may be associated with the
402 barriers that the Andes create with precipitation and humidity and differently from what was presented by
403 Haghtalab et al. (2020).

404 This region has shown changes in precipitation behavior over time, and as discussed by Donat et
405 al. (2016), the spatiotemporal variability in precipitation across the Amazon Basin is more complex than
406 the common refrain of "wet gets wetter and dry gets drier".

407 The average trend for this region is positive (3.24 mm/year), i.e., In a 10-year estimate, the
408 precipitation trend for this region increased by 32.40 mm, which is representative of hydrological terms.

409 This indicates that increasing frequencies of heavy rainy days are strongly related to increases in
410 total annual precipitation, as cited by Haylock et al. (2006). Analysis of the time series for this region

411 indicates that in 1982, the mean annual precipitation was just over 2,000 mm, and in 2018, it was
412 estimated to be close to 2,100 mm.

413 Analyzing the formation of RH 3, located in the subbasins of the Trombetas, Tapajós, Xingu and
414 Negro rivers, it presented a variation of Sen's slope between 1.78 mm/year and 18.69 mm/year, not
415 having negative trend values at any point in this region, an average annual precipitation of 2,177.83 mm
416 and average elevation of 138.57 meters; thus, the least elevated of all regions.

417 It is possible to observe an accentuated positive trend line for this region, a fact represented in
418 the results of Sen's slope statistic tests, with an average trend of 10.38 mm/year.

419 Despite presenting a high annual trend value, it was still the second with the highest trend within
420 the hydrographic basin. However, although the indices had high precipitation averages, this area has
421 already suffered from severe droughts in 1983 and 1992 (Davidson et al. 2012), when, according to
422 Grimm and Zilli (2009), the changes in rainfall variability were probably linked to ENSO and other
423 global phenomena, such as SST anomalies in the Southern Tropical Atlantic, the South American low-
424 level jet and the South American Convergence Zone, which affect the rainfall in the western part of the
425 basin and are currently exhibiting greater variability (Liebmann et al. 2004).

426 Homogeneous Region 4 is present in the northern Amazon River Basin, mostly in the subbasin
427 of the Negro River and part of the subbasins of the Solimões and Madeira Rivers. This study presented
428 results of Sen's slope varying from -2.97 mm/year to 11.28 mm/year, with annual precipitation averages
429 of 2,657.22 mm (largest region in rainfall indices) and an average elevation of 155 meters.

430 In this region, the annual rainfall averages were high, and according to the results of Sen's slope
431 test, the trend was increasing, with a rate of 2.73 mm/year, which could make the rainy days even longer.
432 Factors related to the convergence zones, however, include not only these factors, such as the Hadley and
433 Walker circulations, which are associated with a prolongation of the dry season in South America
434 (Agudelo et al. 2018).

435 It is precisely for this reason that moisture is displaced toward the interior, causing the moisture
436 trends over much of the Amazon Basin to be influenced by a strengthening of the Walker circulation
437 (Barichivich et al. 2018), which were identified in the northern and western parts of the basin.

438 In the case of homogeneous Region 5, which was present in part of the Solimões River subbasin
439 and part of the Madeira River subbasin, it presented a variation in Sen's slope between 10.93 mm/year
440 and 43.67 mm/year, presenting no negative trend values. This region presented an average annual
441 precipitation of 2,368.52 mm, together with an average elevation of 197 meters.

442 The precipitation trend line in this region is well accentuated, a fact that is justified by the results
443 presented by Sen's slope estimator, giving a positive result of 19.81 mm/year.

444 However, despite the positive results, near Porto Velho, Roraima-Brazil, this region presents a
445 "diagonal pattern" of decreasing precipitation in the region, but it was not associated with deforested
446 regions or other major changes in surface cover (Haghtalab et al. 2020).

447 This structure, which is evident in Silva et al. (2018), has lower significance, and this diagonal
448 pattern of drying shows spatial similarity with correlations of rainfall with the South Atlantic TSM (Yoon
449 and Zeng 2010).

450 However, around Iquitos, Peru, Haghtalab et al. (2020) found a mean annual precipitation with
451 an increase of 10.8 mm/day over the 37 years of study, with a clear trend, with erratic behavior in extreme
452 dry season events. Most of the increase was due to extreme rainy season events (18 additional events over
453 37 years).

454 Finally, the formation of homogeneous Region 6 (mouth of the Amazon River is present in this
455 region) is situated mostly in the subbasins of the Tapajós and Xingu Rivers and a part in the subbasins of
456 the Madeira and Trombetas Rivers.

457 This region has a Sen's slope variation between -22.74 mm/year and 7.86 mm/year, with an
458 average annual precipitation of 1,975.93 mm and an average elevation of 279 meters.

459 The precipitation trends for this region are negative according to the results of Sen's slope test,
460 with an average trend of -0.62 mm/year. These results reinforce the hypothesis that at the mouth of the
461 Amazon River, there is a tendency for precipitation to decrease.

462 Nogueira (2008) states that some precipitation anomalies may have influenced this region, where
463 the length of the dry season increased in most regions east of the basin to 9 months (Li et al. 2006).

464 However, correlations with other factors make the results more complex. For example, the
465 eastern region is highly influenced by ENSO (Marengo 2004; Coe et al. 2009), and the long dry season is
466 also driven by subsidence connected to the ITCZ (Fu et al. 2001) and SSTs (Yoon and Zeng 2010).

467 **4. CONCLUSION**

468 The behavior of rainfall in the Amazon River Basin is constantly changing, where most of the
469 Amazon area has undergone climatic changes. In general, the western regions tend to be wetter, while the
470 eastern and southern regions tend to be drier.

471 In the collection and analysis of data, it was found that the GPCC meteorological satellite data
472 were fundamental and valid for the information obtained in this study and can be used in new
473 climatological analyses, as well as the applicability of the tests used in the formation of homogeneous
474 regions (fuzzy C-means), validating the groups by the indices of validations because they managed to
475 form distinct groups, with precipitation averages and well-defined trends and with a spatialization of the
476 regions consistent with several studies presented in this manuscript.

477 To the best of our knowledge, this is one of the few studies to form homogeneous regions of
478 precipitation trends for the Amazon River Basin using high temporal and spatial resolution data.

479 The drivers of the spatial pattern of climate and its variability are complicated in the basin. There
480 are no water limitations thus far for the region; however, regions showing negative trends of precipitation
481 in recent years were observed, which may change the excellent water pattern of the region.

482 The applicability of the three nonparametric tests demonstrated that there are different
483 precipitation trends in the basin depending on the area. The central portion of the basin, toward the south,
484 presented negative precipitation tendencies according to the methods, a fact that can be related to the Arc
485 of Deforestation in Legal Amazonia, where the removal of native vegetation can be causing a decrease in
486 precipitation in the area, affecting the local climate. In all three tests, the mouth of the Amazon River
487 showed a negative trend in precipitation.

488 **5. STATEMENTS & DECLARATIONS**

489 **5.1. Funding**

490 This manuscript was supported by Master's scholarship no. 88882.445051/2019-01, funded by
491 the Coordination for the Improvement of Higher Level Personnel - CAPES for Author A. Author B did
492 not receive any grant for the development of the article.

493 **5.2. Competing Interests**

494 The authors A and B have no financial interests or conflicts of interest on this manuscript.

495 **5.3. Ethics approval and consent to participate**

496 The authors declare that this manuscript is in accordance with the ethical responsibilities of the
497 journal and the Committee on Publication Ethics (COPE).

498 **5.4. Consent for publication**

499 The authors agree with the contents of this manuscript and have all given consent for
500 submission, as well as obtained the consent of the responsible authorities of the institute/organisation
501 where the work was carried out.

502 **5.5. Author Contributions**

503 All authors contributed to the design and development of the study. The preparation of the
504 material, data collection and data analysis were performed by Authors A and B, David Figueiredo
505 Ferreira Filho and Francisco Carlos Lira Pessoa. The first version of the manuscript was written by David
506 Figueiredo Ferreira Filho and both revised the final text. Author B, Francisco Carlos Lira Pessoa, applied
507 the methodology of the work and Author A, David Figueiredo Ferreira Filho, discussed the results.
508 Authors A and B made the conclusion of the work. All authors read and approved the final manuscript.

509 **5.6. Data Availability**

510 The datasets generated during and analysed during the current study are available on the DWD
511 website and can be accessed via the link: <https://kunden.dwd.de/GPCC/Visualizer>.

512 **5.7. Acknowledgements**

513 The authors would like to thank everyone who indirectly participated in the construction of this
514 research.

515 6. REFERENCES

516 Abdul, A. O.; Burn D. Trends and variability in the hydrological regime of the Mackenzie River Basin.
517 *Journal of Hydrology*, 319 (2006): 282–29. DOI: 10.1016/j.jhydrol.2005.06.039, 2006.

518 Aceituno, P. On the functioning of the southern oscillation in the South American sector. Part I: surface
519 climate. *Monthly Weather Review*, 116.3 (1988): 505-524.

520 Aguado, A. G.; Cantanhede, M. A. Lógica Fuzzy. Available in: <
521 http://www.sysrad.com.br/redmine/attachments/1843/Artigo_logicaFuzzi.pdf > (2010).

522 Agudelo J, Arias PA, Vieira SC, Martínez JA. Influence of longer dry seasons in the southern Amazon on
523 patterns of water vapour transport over northern South America and the Caribbean. *Clim Dyn*, 52.5
524 (2018):1–19. <https://doi.org/10.1007/s00382-018-4285-1>

525 Almeida TDC, Oliveira-Júnior JF, Cubo P. Spatiotemporal rainfall and temperature trends throughout the
526 Brazilian legal Amazon, 1973-2013: rainfall and temperature trends throughout the Brazilian legal
527 Amazon. *Artic Int J Climatol.*, 37. 4 (2017): 2013-2026. <https://doi.org/10.1002/joc.4831>

528 Arvor D, Funatsu BM, Michot V, Dubreui V. Monitoring rainfall patterns in the southern amazon with
529 PERSIANN-CDR data: longtermcharacteristics and trends. *Remote Sens* 9.9 (2017).
530 <https://doi.org/10.3390/rs9090889>.

531 Arvor, Damien, et al. Monitoring rainfall patterns in the southern amazon with PERSIANN-CDR data:
532 Long-term characteristics and trends. *Remote Sensing*, 9.9 (2017): 889.

533 Asfaw, A.; Simane, B.; Hassen, A.; Batinder, A. Variability and time series trend analysis of rainfall and
534 temperature innorthcentral Ethiopia: A case study in Woleka sub-basin. *Weather and Climate Extremes*,
535 19 (2018): 29-41.

536 Barichivich J, Gloor E, Peylin P, Brienen RJW, Schöngart J, Espinoza JC, Pattnayak KC. Recent
537 intensification of Amazon flooding extremes driven by strengthened Walker circulation. *Sci Adv*, 4.9
538 (2018). <https://doi.org/10.1126/sciadv.aat8785>

539 Bezdek, J. C.; Pal, S. K. Fuzzy models for pattern recognition: methods that search for structures in data.
540 *Methods that search for structures in data.* IEEE Press, New York. (1992).

541 Bezdek, J. C. Cluster validity with fuzzy sets. *Journal of Cybernetics* 3 (1974b): 58–74.

542 Bezdek, J. C. Numerical taxonomy with fuzzy sets. *Journal of Mathematical Biology* 1 (1974a): 57–71.

543 Bezdek, J. C. Pattern recognition with fuzzy objective function algorithms. Plenum Press, New York
544 (1981).

545 Bezdek, J. C., Trivedi, M., Ehrlich, R., And Full, W. Fuzzy clustering; a new approach for geostatistical
546 analysis. *Int. Jour. Sys., Meas., and Decisions.* (1982).

547 Bloch, I. Fuzzy spatial relationships for image processing and interpretation: a review. *Image and Vision*
548 *Computing*, 23 (2005): 89-110.

549 Braga, R.R.; Bornatowski, H.; Vitule, J.R.S. Feeding ecology of fishes: an overview of worldwide
550 publications. *Reviews in Fish Biology and Fisheries*, 22 (2012): 915–929.

551 Campos, I. de O. Referencial Altimétrico para a bacia do Rio Amazonas. Tese (Doutorado em Engenharia
552 de Transportes). Escola Politécnica da Universidade de São Paulo- USP-SP, São Paulo, 2004.

553 Correa, S.B.; Winemiller, K.O. Niche partitioning among frugivorous fishes in response to fluctuating
554 resources in the Amazonian floodplain forest. *Ecology*, 95 (2014): 210–224.

555 Costa MH, Pires GF. Effects of Amazon and Central Brazil deforestation scenarios on the duration of the
556 dry season in the arc of deforestation. *Int J Climatol* 30.13 (2010): 1970–1979.
557 <https://doi.org/10.1002/joc.2048>.

558 CPTEC, Centro de Previsão de Tempo e Estudos Climáticos. Disponível em:
559 <<http://www1.cptec.inpe.br/products/elinho/elinho3p.html>>. (1998).

560 Davidson EA, De Araújo AC, Artaxo P, Balch JK, Brown IF, Mercedes MM et al. The Amazon basin in
561 transition. *Nature* 481.7381 (2012): 321–328. <https://doi.org/10.1038/nature10717>.

- 562 Davies, David L., and Donald W. Bouldin. A cluster separation measure. *IEEE transactions on pattern*
563 *analysis and machine intelligence* 2 (1979): 224-227.
- 564 Debortoli NS, Dubreuil V, Funatsu B, Delahaye F, Henke De Oliveira C, Rodrigues-Filho S et al.
565 Rainfall patterns in the Southern Amazon: a chronological perspective (1971-2010). *Clim Chang* 132
566 (2015): 251–264. <https://doi.org/10.1007/s10584-015-1415-1>.
- 567 Delahaye, F.; Kirstetter, P.-E.; Dubreuil, V.; Machado, L.A.T.; Vila, D.; Clark, R. A consistent gauge
568 database for daily rainfall analysis over the Legal Brazilian Amazon. *J. Hydrol.*, 527 (2015): 292–304.
- 569 Donat MG, Lowry AL, Alexander LV, O’Gorman PA, Maher N. More extreme precipitation in the
570 world’s dry and wet regions. *Nat Clim Chang* 6.5 (2016):508–513. <https://doi.org/10.1038/nclimate2941>
- 571 Dunn, J. C. A Fuzzy Relative of the ISODATA Process and Its Use in Detecting Compact Well-Separated
572 Clusters. *Journal of Cybernetics*, 3.3 (1973): 32–57.
- 573 Ely, D. F.; Dubreuil, V. Análise das Tendências Espaço-Temporais das precipitações anuais para o Estado
574 do Paraná – Brasil. *Revista Brasileira de Climatologia*, 13.21 (2017).
- 575 Ferrari, A. L. Variabilidade e tendência da temperatura e pluviosidade nos municípios de Pirassununga,
576 Rio Claro, São Carlos e São Simão (SP): Estudo sobre mudança climática de curto prazo em escala local.
577 Tese. Universidade de São Paulo - USP. São Carlos/SP, (2012): 156.
- 578 Filizola, J. N. P. O fluxo de sedimentos em suspensão nos rios da Bacia Amazônica brasileira. ANEEL,
579 Brasília, Brasil. (1999).
- 580 Fu R, Dickinson RE, Chen M, Wang H, Fu R, Dickinson RE, ... Wang H. How do tropical sea surface
581 temperatures influence the seasonal distribution of precipitation in the equatorial Amazon? *J Clim*, 14.20
582 (2001): 4003–4026. [https://doi.org/10.1175/1520-0442\(2001\)014<4003:HDTSSST>2.0.CO;2](https://doi.org/10.1175/1520-0442(2001)014<4003:HDTSSST>2.0.CO;2)
- 583 Funatsu BM, Dubreuil V, Claud C, Arvor D, GanMA. Convective activity in Mato Grosso state (Brazil)
584 from microwave satellite observations: comparisons between AMSU and TRMM data sets. *J Geophys*
585 *Res Atmos.*, 117.16 (2012):1–16. <https://doi.org/10.1029/2011JD017259>.
- 586 Funk, C.; Verdin, A.; Michaelsen, J.; Peterson, P.; Pedreros, D.; Husak, G. A global satellite-assisted
587 precipitation climatology. *Earth Syst. Sci. Data*, 7 (2015): 275–287.
- 588 Getirana, Augusto CV, et al. Assessment of different precipitation datasets and their impacts on the water
589 balance of the Negro River basin. *Journal of Hydrology* 404.3-4 (2011): 304-322.
- 590 Gomes, E. P.; Blanco, C. J.C.; Pessoa, F. C. L. P. Regionalization of precipitation with determination of
591 homogeneous regions via fuzzy c-means. *Brazilian Journal of Water Resources*, 23.51 (2018).
592 <https://doi.org/10.1590/2318-0331.231820180079>.
- 593 Grimm AM, Zilli MT. Interannual variability and seasonal evolution of summer monsoon rainfall in
594 South America. *J Clim* 22.9 (2009): 2257–2275. <https://doi.org/10.1175/2008JCLI2345.1>
- 595 Haghtalab, N., Moore, N., Heerspink, B. P., & Hyndman, D. W. Evaluating spatial patterns in
596 precipitation trends across the Amazon basin driven by land cover and global scale forcings. *Theoretical*
597 *and Applied Climatology*, 1.17 (2020).
- 598 Halkidi, M.; Batistakis, Y.; Vargiannis, M. Cluster validity methods: Part. I. *ACM SIGMOD Record*,
599 31.2 (2002).
- 600 Haylock MR, Peterson TC, Alves LM, Ambrizzi T, Anunciação YMT, Baez J et al. Trends in Total and
601 extreme south American rainfall in 1960–2000 and links with sea surface temperature. *J Clim* 19.8
602 (2006):1490–1512. <https://doi.org/10.1175/JCLI3695.1>
- 603 Hirsch, R.M.; Slack, J.R. A nonparametric trend test for seasonal data with serial dependence. *Water*
604 *Resources Research*, 20 (1984): 727-732.
- 605 Hosseini, A., Ghavidel, Y., Khorshiddoust, A. M., and Farajzadeh, M. Spatio-temporal analysis of dry
606 and wet periods in Iran by using Global Precipitation Climatology Center-Drought Index (GPCC-DI).
607 *Theoretical and Applied Climatology*, 1.11 (2020).
- 608 INPE, Instituto Nacional de Pesquisas Espaciais. PRODES survey 2004. INPE, São José dos Campos,
609 Brazil. (2004).

- 610 Ishihara, J. H.; Fernandes, L. L.; Duarte, A. A. A. M.; Duarte, A. R. C. L. M.; Ponte, M. X.; Loureiro, G.
611 E. Quantitative and Spatial Assessment of Precipitation in the Brazilian Amazon (Legal Amazon) - (1978
612 to 2007). *Revista Brasileira de Recursos Hídricos*, v. 19 (2014): 29-39.
- 613 Jané, D. De A. An introduction to the study of fuzzy logic. *Journal of Humanities and Applied Social
614 Sciences*, 2 (2004): 1–16.
- 615 Jimenez, K. Q.; Collischonn, W.; Paiva, R. C. D.; Buarque, D. C. Comparison of rain estimate products
616 by remote sensing using a hydrological model in the Amazon River basin. 4th Ibam Cientific Meeting
617 (2011).
- 618 Kendall, M. G. *Rank Correlation Methods*. Charles Griffin. London (1975).
- 619 Khanna J, Medvigy D, Fueglistaler S, Walko R. Regional dryseason climate changes due to three decades
620 of Amazonian deforestation. *Nat Clim Chang* 7.3 (2017): 200–204. <https://doi.org/10.1038/nclimate3226>.
- 621 Laurance WF, Lovejoy TE, Vasconcelos HL, Bruna EM, Didham RK, Stouffer PC, ... John Heinz H.
622 Ecosystem decay of Amazonian forest fragments: a 22-year investigation. *Conserv Biol* 16.3 (2002):605–
623 618.
- 624 Leite, R.G.; Silva, J.V.V.; Freitas, C.E. Abundance and distribution of fish larvae in Lake Catalão and in
625 the encounter of the Solimões and Negro rivers, Amazonas, Brazil. *Acta Amazonica*, 36 (2006): 557-562.
- 626 Li W, Fu R, Dickinson RE. Rainfall and its seasonality over the Amazon in the 21st century as assessed
627 by the coupled models for the IPCC AR4. *J Geophys Res Atmos* 111.2 (2006): 1–14.
628 <https://doi.org/10.1029/2005JD006355>
- 629 Liebmann B, Kiladis GN, Vera CS, Saulo AC, Carvalho LMV. Subseasonal variations of rainfall in South
630 America in the vicinity of the low-level jet east of the Andes and comparison to those in the South
631 Atlantic convergence zone. *J Clim* 17.19 (2004): 3829–3842. [https://doi.org/10.1175/1520-0442\(2004\)017<3829:SVORIS>2.0.CO;2](https://doi.org/10.1175/1520-0442(2004)017<3829:SVORIS>2.0.CO;2)
- 633 Limberger, L., and M. E. S. Silva. Precipitation observed in the Brazilian Amazon: comparison between
634 conventional network data and NCEP/NCAR, CRU and GPCC reanalysis I data. *Brazilian Journal of
635 Climatology* 22 (2018): 20-37.
- 636 LIRA, Bruna Roberta Pereira et al. Avaliação do comportamento e da tendência pluviométrica na
637 Amazônia Legal no período de 1986 a 2015. Dissertação de mestrado do curso de pós-graduação em
638 Engenharia Civil. Belém-Pa. (2019).
- 639 Longobardi P, Montenegro A, Beltrami H, Eby M. Deforestation induced climate change: effects of
640 spatial scale. *PLoS One* 11(4). <https://doi.org/10.1371/journal.pone.0153357>.
- 641 Loureiro, G.E.; Fernandes, L.L.; Ishihara, J.H. Spatial and temporal variability of rainfall in the
642 Tocantins-Araguaia hydrographic region. *Acta Scientiarum*, 37.1 (2016): 89-98.
- 643 Mann, H. B. Nonparametric tests against trend. *Econometrica. Journal of the Econometric Society*,
644 (1945): 245-259.
- 645 Marengo JA. Interdecadal variability and trends of rainfall across the Amazon basin. *Theor Appl Climatol*
646 78.1–3 (2004): 79–96. <https://doi.org/10.1007/s00704-004-0045-8>.
- 647 Marengo JA, Espinoza JC. Extreme seasonal droughts and floods in Amazonia: causes, trends and
648 impacts. *Int J Climatol* 36.3 (2016): 1033– 1050. <https://doi.org/10.1002/joc.4420>.
- 649 Marengo, J. A., Tomasella, J., Alves, L. M., Soares, W. R., And Rodriguez, D. A. The drought of 2010 in
650 the context of historical droughts in the Amazon region. *Geophys. Res. Lett.*, 38.12 (2011).
651 Doi:10.1029/2011GL047436, 2011.
- 652 Marengo, J.; Hastenrath, S. Case studies of extreme climatic events in the Amazon basin. *Journal of
653 Climate*, 6.4 (1993): 617-627.
- 654 Marengo, J.A.; Liebman, B.; Wainer, L.; Kousky, V.E. On the characteristics of onset and demise of the
655 rainy season in amazonia. *Journal of Climate* (2000).
- 656 Menezes, F. P.; Fernandes, L. L.; Analysis of precipitation trends and variability in the state of Pará.
657 *Encyclopedia Biosphere*, 13.24 (2016): 1580.

- 658 Monte-Mor, R. L. Extended urbanization and settlement patterns: an environmental approach. Pages 109-
659 120 in N. Brenner, editor. Implosions/explosions: towards a study of planetary urbanization. Jovis, Berlin,
660 Germany. (2013).
- 661 Mortillaro, Jean-Michel et al. Trophic opportunism of floodplain fish in central Amazonia. *Freshwater*
662 *Biology*, 60.8 (2015): 1659-1670.
- 663 Nascimento, S.; Mirkin, B.; Moura-Pires, F. A fuzzy clustering modelo f data and fuzzy c-means. The
664 Nineth IEEE International Conference on Fuzzy Systems: Soft Computing in the Information Age,
665 (2000): 302-307.
- 666 Nogueira, V. Da S. Interannual variability of precipitation at the mouth of the Amazon River. Master's
667 thesis of the graduate course in meteorology. São José dos Campos: INPE, (2008): 134.; (INPE-15348-
668 TDI/1384)
- 669 Pakhira M. K., Bandyopadhyay S., Maulik K. Validity index for crisp and fuzzy clusters, *Pattern*
670 *Recognition* 37 (2004): 481-501.
- 671 Pandey, B.K.; Khare, D. Identification of trend in long term precipitation and reference
672 evapotranspiration over Narmada river basin (India). *Global and Planetary Change*, v. 161 (2018): 172–
673 82.
- 674 Partal, T.; Kahya, E. Trend analysis in Turkish precipitation data. *Hydrological processes*, 20.9 (2006):
675 2011-2026.
- 676 Pedrycz, W.; Vukovich, G. Fuzzy clustering with supervision. *Pattern Recognition. The Journal of the*
677 *Pattern Recognition Society*, 37 (2004): 1339-1349.
- 678 Portela, M.M.; Quintela, A.C.; Santos, J.F.; Vaz, C; Martins, C. Trends in time series of hydrological
679 variables. *Portuguese Association of Water Resources (APRH)*, 32.1 (2011): 43-60.
- 680 Prudente, B. S; Carneiro-Marinho, P; Valente, R.M; Montag, L.F.A. Feeding ecology of *Serrasalmus*
681 *gouldingi* (Characiformes: Serrasalminidae) in the lower Anapu River region, Eastern Amazon, Brazil. *Acta*
682 *Amazonica*, 46.3 (2016): 259-270.
- 683 Ronchail, J.; Cochonneau, G.; Molinier, M.; Guyot, J.L.; Chaves, A.G.D.M.; Guimarães, V.; De Oliveira,
684 E. Interannual rainfall variability in the Amazon basin and sea-surface temperatures in the equatorial
685 Pacific and the tropical Atlantic Oceans. *Int. J. Clim.*, 22 (2002): 1663–1686.
- 686 Rousseeuw, Peter J. Silhouettes: a graphical aid to the interpretation and validation of cluster analysis.
687 *Journal of computational and applied mathematics*, 20 (1987): 53-65. [https://doi.org/10.1016/0377-
688 0427\(87\)90125-7](https://doi.org/10.1016/0377-0427(87)90125-7).
- 689 Rustemeier, E., Ziese, M., Meyer-Christoffer, A., Schneider, U., Finger, P., & Becker, A.. Uncertainty
690 Assessment of the ERA-20C Reanalysis Based on the Monthly In Situ Precipitation Analysis of the
691 Global Precipitation Climatology Centre. *Journal of Hydrometeorology* 20.2 (2019): 231-250.
- 692 Salviano MF, Daniel Groppo J, Pellegrino GQ. Trends analysis of precipitation and temperature data in
693 Brazil. *Rev Brasil Meteorol* 31.1 (2016):64–73. <https://doi.org/10.1590/0102-778620150003>.
- 694 Sánchez-Botero, J.I.; Araújo-Lima, A.C.R.M. As macrófitas aquáticas como berçário para a ictiofauna da
695 várzea do rio Amazonas. *Acta Amazonica*, 31 (2001): 437-447.
- 696 Satyamurty P, de Castro AA, Tota J, da Silva Gularte LE, Manzi AO. Rainfall trends in the Brazilian
697 Amazon Basin in the past eight decades. *Theor Appl Climatol.*, 99.1–2 (2010): 139–148.
698 <https://doi.org/10.1007/s00704-009-0133-x>.
- 699 SCHEFF, S. W. Chapter 8 Nonparametric Statistics. University of Kentucky SanderseBrown Center on
700 Aging, Lexington, KY, USA. (2016). Available in:
701 <https://www.sciencedirect.com/science/article/pii/B9780128047538000087>.
- 702 Schneider, U., Becker, A., Finger, P. et al. GPCC's new land surface precipitation climatology based on
703 quality-controlled in situ data and its role in quantifying the global water cycle. *Theor Appl Climatol* 115
704 (2014): 15–40. <https://doi.org/10.1007/s00704-013-0860-x>.
- 705 Schneider, U.; Becker, A.; Meyer-Christoffer, A.; Rudolf, B. Global Precipitation Analysis Products of
706 the GPCC. Global Precipitation Climatology Centre (GPCC) Deutscher Wetterdienst, Offenbach a. M.,
707 Germany. (2011).

708 Schneider, U.; Finger, P.; Meyer-Christoffer, A.; Rustemeier, E.; Ziese, M.; Becker, A. Evaluating the
709 Hydrological Cycle over Land Using the Newly-Corrected Precipitation Climatology from the Global
710 Precipitation Climatology Centre (GPCC). *Atmosphere*, v. 8.52 (2017). DOI:10.3390/ATMOS8030052

711 Sen, P. K. Estimates of the regression coefficient based on Kendall's tau. *Journal of the American*
712 *statistical association*,63.324 (1968): 1379-1389.

713 Silva CHL Jr, Almeida CT, Santos JRN, Anderson LO, Aragão LEOC, Silva FB; Spatiotemporal rainfall
714 trends in the Brazilian legal Amazon between the years 1998 and 2015. *Water (Switzerland)*, 10.9 (2018):
715 1–16. <https://doi.org/10.3390/w10091220>.

716 Silva, M. Do S. R. *Bacia Hidrográfica do Rio Amazonas: Contribution to Framework and Preservation.*
717 Thesis (Doctorate in Chemistry). Postgraduate Degree in Chemistry, Federal University of Amazonas –
718 UFAM, Amazonas (2013).

719 Song, X. P., Huang, C., Saatchi, S. S., Hansen, M. C., & Townshend, J. R. Annual carbon emissions from
720 deforestation in the Amazon Basin between 2000 and 2010. *PloS one*, 10.5 (2015).

721 Tan, P. N.; Steinbach, M.; Kumar, V. *Introduction to Data Mining.* Addison Wesley. (2005).

722 Tao, H.; Fraederich, K.; Menz, C.; Zhai, J. Trends in extreme temperature indices in the Poyang Lake
723 Basin, China. *Stoch. Environ. Res. Risk Asses.*, 28 (2014): 1543-1553.

724 Tejadas et al. 271 Report of the Intergovernmental Panel on Climate Change. Cambridge, University
725 Press, (2013): 1535.

726 TEJADAS, B.E; BRAVO, J.M; SANAGIOTTO, D.G; TASSI, R E MARQUES, D,M,L,M. Projections of
727 inflows to the Mango Lagoon based on climate change scenarios. *Brazilian Journal of Meteorology*, 31.3
728 (2016): 262-272.

729 Tomasella, J.; Pinho, P. F.; Borma, L. S. E.; Marengo, J. A. The droughts of 1997 and 2005 in Amazonia:
730 floodplain hydrology and its potential ecological and human impacts. *Climatic change*, 116 (2013): 723-
731 746.

732 Villar, Espinoza; Jhan, Carlo, et al. Spatio-temporal rainfall variability in the Amazon basin countries
733 (Brazil, Peru, Bolivia, Colombia, and Ecuador). *International Journal of Climatology: A Journal of the*
734 *Royal Meteorological Society* 29.11 (2009): 1574-1594. doi: 10.1002/joc.1791.

735 Walker R, Moore NJ, Arima E, Perz S, Simmons C, Caldas M,Vergara D, Bohrer, C. Protecting the
736 Amazon with protected areas. *Proceedings of the National Academy of Sciences of the United States of*
737 *America* 106.26 (2009):10582–10586. <https://doi.org/10.1073/pnas.0806059106>.

738 WMO. *Guide to Meteorological Instruments and Methods of Observation*; WMO: Geneva, Switzerland,
739 (2008).

740 Xie, XL and Beni, G. A validity measure for fuzzy clustering. *IEEE Transactions on Pattern Analysis and*
741 *Machine Intelligence* 13.4 (1991):841–846.

742 XU, R. E WUNSCH, D. II survey of clustering algorithms. *IEEE Transactions on Neural Networks* 16.3
743 (2005): 645-678.

744 Yoon JH, Zeng N. An Atlantic influence on Amazon rainfall. *Clim Dyn* 34.2 (2010): 249–264.
745 <https://doi.org/10.1007/s00382-009-0551-6>

746 Zadeh, L.A. Fuzzy sets. *Information and Control. California - USA.* 8 (1965): 338-353.